Solid-State ^{13}C NMR Chemical Shift Anisotropy Tensors of Polypeptides

Yufeng Wei, Dong-Kuk Lee, and A. Ramamoorthy*

Contribution from the Biophysics Research Division, Department of Chemistry, and Macromolecular Science and Engineering, The University of Michigan, Ann Arbor, Michigan 48109-1055

Received January 17, 2001. Revised Manuscript Received April 25, 2001

Abstract: Carbon-13 chemical shift anisotropy (CSA) tensors for various carbon sites of polypeptides, and for carbon sites in α-helical and β-sheet conformations of poly-L-alanine, and polyglycine, are presented. The carbonyl ^{13}C CSA tensors were determined from one-dimensional CPMAS spectra obtained at a slow spinning speed, whereas the CSA tensors of C_α and other carbons in side chains of peptides were determined using 2D PASS experiments on powder samples. The results suggest that the spans of ^{13}Carbonyl CSA tensors of alanine and glycine residues in various peptides are similar, even though the magnitude of individual components of the CSA tensor and the isotropic chemical shift are different. In addition, the δ_{22} element is the only component of the ^{13}Carbonyl CSA tensor that significantly depends on the CO···HN hydrogen-bond length. Solid-state NMR experimental results also suggest that ^{13}Carbonyl and $^{13}C_\alpha$ CSA tensors are similar for α-helical and β-sheet conformations of poly-L-alanine, which is in agreement with the reported quantum chemical calculation studies and previous solid-state NMR experimental studies on other systems. On the other hand, the $^{13}C_\alpha$ CSA tensor of the first alanine residue is entirely different from that of the second or later alanine residues of the peptide. While no clear trends in terms of the span and the anisotropic parameter were predicted for $^{13}C_\beta$ CSA tensors of alanine, they mainly depend on the conformation and dynamics of the side chain as well as on the packing interactions in the solid state of peptides.

Introduction

The structure determination of insoluble proteins such as membrane-associated proteins, fibrous proteins, and protein aggregates is an important and challenging problem in biochemistry. Most of such systems have been inaccessible to the more traditional physical techniques such as X-ray diffraction, because of its requirement for single-crystal samples, and such as liquid-state NMR spectroscopy, because of its requirements for relatively low-molecular weight, rapidly reorienting proteins. The recent few years have witnessed extensive application of solid-state NMR spectroscopy to investigate noncrystalline and disordered biological solids, because it does not have limits on the molecular size, tumbling, and disorder.[1,2] Also, it is possible to describe the structure and dynamics of noncrystalline systems in an integrated manner using solid-state NMR methods. The interpretation of most solid-state NMR experimental results from such insoluble proteins requires well-characterized chemical shift anisotropy (CSA) tensors.[1−5] However, unfortunately, only very few accurate ^{13}C CSA tensors are available in the literature for the structural studies of peptides and proteins.[6−9] Therefore, there is a significant interest in accurately determined ^{13}C CSA tensors from peptides and proteins. Also, it is important to understand the variation of ^{13}C CSA tensors with respect to amino acid residue, secondary structure, hydrogen bonding, and solvation.

Since the magnitudes and orientations of the CSA tensor are known to be intimately related to the local environment around the nuclei,[10] CSA tensors are useful to gain insight into the conformation and dynamics of the backbone as well as the side chain of a protein.[11] On the basis of solid-state NMR studies on single crystals[6,9] and powder samples[7,8,12−15] of peptides and on the basis of liquid-state NMR of proteins[16−25] ^{13}C CSA

* To whom correspondence should be addressed.

(1) Smith, S. O.; Aschheim, K.; Groesbeek, M. *Q. Rev. Biophys.* **1996**, *29*, 395−449.
(2) Fu, R. Q.; Cross, T. A. *Annu. Rev. Biophys. Biomol. Struct.* **1999**, *28*, 235−268.
(3) Lee, D. K.; Wittebort, R. J.; Ramamoorthy, A. *J. Am. Chem. Soc.* **1998**, *120*, 8868−8874.
(4) Lee, D. K.; Santos, J. S.; Ramamoorthy, A. *J. Phys. Chem. B* **1999**, *103*, 8383−8390.
(5) Brender, J. R.; Taylor, D. M.; Ramamoorthy, A. *J. Am. Chem. Soc.* **2001**, *123*, 914−922.
(6) Harbison, G. S.; Jelinski, L. W.; Stark, R. E.; Torchia, D. A.; Herzfeld, J.; Griffin, R. G. *J. Magn. Reson.* **1984**, *60*, 79−82.
(7) Oas, T. G.; Hartzell, C. J.; McMahon, T. J.; Drobny, G. P.; Dahlquist, F. W. *J. Am. Chem. Soc.* **1987**, *109*, 5956−5962.
(8) Hartzell, C. J.; Whitfield, M.; Oas, T. G.; Drobny, G. P. *J. Am. Chem. Soc.* **1987**, *109*, 5966−5969.
(9) Takeda, N.; Kuroki, S.; Kurosu, H.; Ando, I. *Biopolymers* **1999**, *50*, 61−69.
(10) deDios, A. C.; Oldfield, E. *Solid State Nucl. Magn. Reson.* **1996**, *6*, 101−125.
(11) Case, D. A. *Curr. Opin. Struct. Biol.* **1998**, *8*, 624−630.
(12) Asakawa, N.; Kuroki, S.; Kurosu, H.; Ando, I.; Shoji, A.; Ozaki, T. *J. Am. Chem. Soc.* **1992**, *114*, 3261−3265.
(13) Teng, Q.; Iqbal, M.; Cross, T. A. *J. Am. Chem. Soc.* **1992**, *114*, 5312−5321.
(14) Kameda, T.; Takeda, N.; Kuroki, S.; Kurosu, H.; Ando, S.; Ando, I.; Shoji, A.; Ozaki, T. *J. Mol. Struct.* **1996**, *384*, 17−23.
(15) Hong, M. *J. Am. Chem. Soc.* **2000**, *122*, 3762−3770.
(16) Dayie, K. T.; Wagner, G. *J. Am. Chem. Soc.* **1997**, *119*, 7797−7806.
(17) Yang, D. W.; Konrat, R.; Kay, L. E. *J. Am. Chem. Soc.* **1997**, *119*, 11938−11940.
(18) Cornilescu, G.; Marquardt, J. L.; Ottiger, M.; Bax, A. *J. Am. Chem. Soc.* **1998**, *120*, 6836−6837.
(19) Lienin, S. F.; Bremi, T.; Brutscher, B.; Bruschweiler, R.; Ernst, R. R. *J. Am. Chem. Soc.* **1998**, *120*, 9870−9879.
(20) Chiarparin, E.; Pelupessy, P.; Ghose, R.; Bodenhausen, G. *J. Am. Chem. Soc.* **1999**, *121*, 6876−6883.

10.1021/ja010145l CCC: $20.00
Published on Web 05/31/2001

tensors have been reported. Magnitudes and orientations of ^{13}C CSA tensors of amide carbonyl carbon from GlyGly, GlyGly·HNO_3, and GlyGly·HCl·H_2O single crystals have been determined.[9] In all of these compounds, the most shielded component, δ_{33}, is perpendicular to the $C_\alpha-C(=O)-N$ plane, the δ_{22} axis lies approximately along the carbonyl bond, and the least shielded component, δ_{11}, is approximately along the direction of the $C(=O)-C_\alpha$ bond.[7−9,26] A large downfield shift for δ_{22} and δ_{iso}, an upfield shift for δ_{11}, and no change for δ_{33} were predicted with a decrease in hydrogen-bond length, $R_{N\cdots O}$.[14] A strong dependence of the ^{13}C CSA tensor of the carboxylate group on hydrogen bonding has also been reported for amino acids and peptides in CPMAS[27,28] and $^1H-^{13}C$ HETCOR experiments.[29] The ^{13}C CSA tensor of amide carbonyl carbon measured from powder samples of several peptides predicted that both the magnitudes and molecular orientation of the principal components vary significantly from molecule to molecule.[7−9,14,26] Quantum chemical calculations[30,31] and liquid-state[16,19,21,23] and solid-state[32,33] NMR experiments have been utilized to correlate the anisotropic chemical shifts and secondary structure in peptides and proteins. On the basis of ^{13}CO CSA studies, it is predicted that the range of δ_{iso} values found in proteins mainly arises from the dependence of δ_{22} on the secondary structure.[14] There are very few studies on $^{13}C_\alpha$ CSA tensors that reported the dependence of $^{13}C_\alpha$ CSA tensors on the secondary structure of proteins.[15,25,33,34] In general, knowledge on the ^{13}C CSA tensors of $^{13}C_\alpha$ and $^{13}C_\beta$ nuclei in the side chains of proteins is essential to study the structure and dynamics of proteins using NMR spectroscopy. In particular, they will be highly useful to interpret the solid-state ^{13}C NMR spectra of membrane-associated proteins embedded in lipid bilayers. Therefore, it is important to analyze ^{13}C CSA tensors associated with various sites of proteins. In this study, ^{13}C CSA tensors of small peptides, poly-L-alanine, and polyglycine samples are presented. The dependence of ^{13}C CSA tensors on the secondary structure is also discussed on the basis of the experimental results. Two-dimensional PASS (phase adjusted spinning sideband) solid-state NMR experiments on powder samples,[35,36] and one-dimensional CPMAS spectra obtained at slow spinning speeds were used to measure the CSA tensors.

Experimental Section

All dipeptide, tripeptide, and polyglycine samples were purchased from Sigma Co. and used without further purification. The commercial poly-L-alanine (21.6 kDa) sample purchased from Sigma Co. was mainly α-helical. It was ground for 30 min in a ball-mill to induce 45% α-helix and 55% β-sheet conformations. The percentage conformations were estimated from ^{13}C CPMAS spectra as explained in our earlier publication.[37] This sample is used to determine the ^{13}C CSA tensors of α-helix and β-sheet conformations.

All solid-state NMR experiments were performed on a Chemagnetics/Varian CMX Infinity 400 MHz spectrometer, operating at a Larmor frequency of 400.139 MHz for ^1H and 100.623 MHz for ^{13}C. A double-resonance MAS probe equipped with a 5-mm PENCIL probehead and 5-mm zirconia rotors were used. A sample spinning speed of 500 ± 1 Hz was used in the 2D PASS experiments, while the high-resolution one-dimensional ^{13}C CPMAS spectra were collected using a spinning speed of 6 kHz. A detailed explanation on the 2D PASS pulse sequence, its performance, a *Mathematica* routine to generate a set of PASS solutions, and the data processing can be found elsewhere.[35,36] Sixteen t_1 increments using the timings given in Table 1 of the original reference[35] were used in the 2D PASS experiments. Additional spectrometer parameters include a recycle delay time of 3 s, a 3.0 μs ^1H 90° pulse, a 3.7 μs 90° ^{13}C pulse, a contact time of 1 ms with an rf field strength of 50 kHz, a ^1H decoupling rf field of about 80 kHz, and an acquisition dimension spectral width of 50 kHz with a digital resolution of 48.8 Hz per point. TPPM proton decoupling was used with a total phase-modulation angle of 15° together with a modulation frequency corresponding to a 170° tip angle.[38] Since the π pulse positions in t_1 set back to their original positions after a full cycle and the t_1-FID forms a full echo, the 16-point experimental t_1 data were replicated to 256 points. After the Fourier transformation in the direct dimension, the 2D spectrum was sheared so as to align all sidebands with the center bands in the indirect dimension of the 2D spectrum. Thus, one-dimensional CSA spinning sideband patterns can be obtained from t_1 slices taken at isotropic chemical shifts in the ω_2 dimension of the 2D spectrum. The magnitudes of the principal elements of the CSA tensor were obtained from the best-fitting simulated spinning sideband pattern for each compound.

All of the data were processed in a Sun Sparc 20 workstation using the Spinsight software. Simulations of the spinning CSA sideband spectra were carried out on a PC using a program written in C++ under GAMMA programming environment.[39] In addition to their CSA interactions, carbonyl carbon and α-carbon in a peptide backbone experience both a $^{13}C-^{14}N$ dipolar (or $^{13}C-^{15}N$ dipolar if the amide nitrogens were isotopically labeled) and a quadrupolar contribution from the directly attached ^{14}N nuclei. Since the ^{14}N quadrupolar contribution has been previously estimated to be negligible (less than 20 Hz at 75 MHz),[40−43] it was not taken into account in the ^{13}C CSA simulations. However, the $^{13}C_\alpha-^{14}N$ dipolar coupling affects the $^{13}C_\alpha$ CSA significantly, as the $^{13}C_\alpha-^{14}N$ dipolar coupling is comparable with the span of $^{13}C_\alpha$ chemical shifts.[13,44] The $^{13}C_\alpha-^{14}N$ dipolar coupling constant of 712.7 Hz ($C_\alpha-N$ bond length of 1.45 Å), and the angles that define the orientation of the $^{13}C_\alpha$ CSA tensor with respect to the $^{13}C_\alpha-^{14}N$ dipolar coupling, $\alpha_C = 47.3°$ and $\beta_C = 71.9°$, were used in the

(21) Pang, Y. X.; Zuiderweg, E. R. P. *J. Am. Chem. Soc.* **2000**, *122*, 4841−4842.
(22) Carlomagno, T.; Maurer, M.; Hennig, M.; Griesinger, C. *J. Am. Chem. Soc.* **2000**, *122*, 5105−5113.
(23) Cornilescu, G.; Bax, A. *J. Am. Chem. Soc.* **2000**, *122*, 10143−10154.
(24) Ottiger, M.; Bax, A. *J. Am. Chem. Soc.* **1997**, *119*, 8070−8075.
(25) Tjandra, N.; Bax, A. *J. Am. Chem. Soc.* **1997**, *119*, 9576−9577.
(26) Asakura, T.; Yamazaki, Y.; Seng, K. W.; Demura, M. *J. Mol. Struct.* **1998**, *446*, 179−190.
(27) Gu, Z. T.; McDermott, A. *J. Am. Chem. Soc.* **1993**, *115*, 4282−4285.
(28) Gu, Z. T.; Zambrano, R.; McDermott, A. *J. Am. Chem. Soc.* **1994**, *116*, 6368−6372.
(29) Gu, Z. T.; Ridenour, C. F.; Bronnimann, C. E.; Iwashita, T.; McDermott, A. *J. Am. Chem. Soc.* **1996**, *118*, 822−829.
(30) deDios, A. C.; Oldfield, E. *J. Am. Chem. Soc.* **1994**, *116*, 11485−11488.
(31) Sulzbach, H. M.; Vacek, G.; Schreiner, P. R.; Glabraith, J. M.; Schleyer, P. V.; Schaffer, H. F. *J. Comput. Chem.* **1997**, *18*, 126−138.
(32) Asakawa, N.; Kurosu, H.; Ando, I.; Shoji, A.; Ozaki, T. *J. Mol. Struct.* **1994**, *317*, 119−129.
(33) Asakawa, N.; Takenoiri, M.; Sato, D.; Sakurai, M.; Inoue, Y. *Magn. Reson. Chem.* **1999**, *37*, 303−311.
(34) Havlin, R. H.; Le, H. B.; Laws, D. D.; deDios, A. C.; Oldfield, E. *J. Am. Chem. Soc.* **1997**, *119*, 11951−11958.
(35) Antzutkin, O. N.; Shekar, S. C.; Levitt, M. H. *J. Magn. Reson. Ser. A* **1995**, *115*, 7−19.
(36) Antzutkin, O. N.; Lee, Y. K.; Levitt, M. H. *J. Magn. Reson.* **1998**, *135*, 144−155.
(37) Lee, D. K.; Ramamoorthy, A. *J. Phys. Chem. B* **1999**, *103*, 271−275.
(38) Bennett, A. E.; Rienstra, C. M.; Auger, M.; Lakshmi, K. V.; Griffin, R. G. *J. Chem. Phys.* **1995**, *103*, 6951−6958.
(39) Smith, S. A.; Levante, T. O.; Meier, B. H.; Ernst, R. R. *J. Magn. Reson. Ser. A* **1994**, *106*, 75−105.
(40) Hexem, J. G.; Frey, M. H.; Opella, S. J. *J. Am. Chem. Soc.* **1981**, *103*, 224−226.
(41) Naito, A.; Ganapathy, S.; McDowell, C. A. *J. Chem. Phys.* **1981**, *74*, 5393−5397.
(42) Zumbulyadis, N.; Henrichs, P. M.; Young, R. H. *J. Chem. Phys.* **1981**, *75*, 1603−1611.
(43) Naito, A.; Ganapathy, S.; McDowell, C. A. *J. Magn. Reson.* **1982**, *48*, 367−381.
(44) Takegoshi, K.; Naito, A.; McDowell, C. A. *Magn. Reson. Chem.* **1986**, *24*, 544−546.

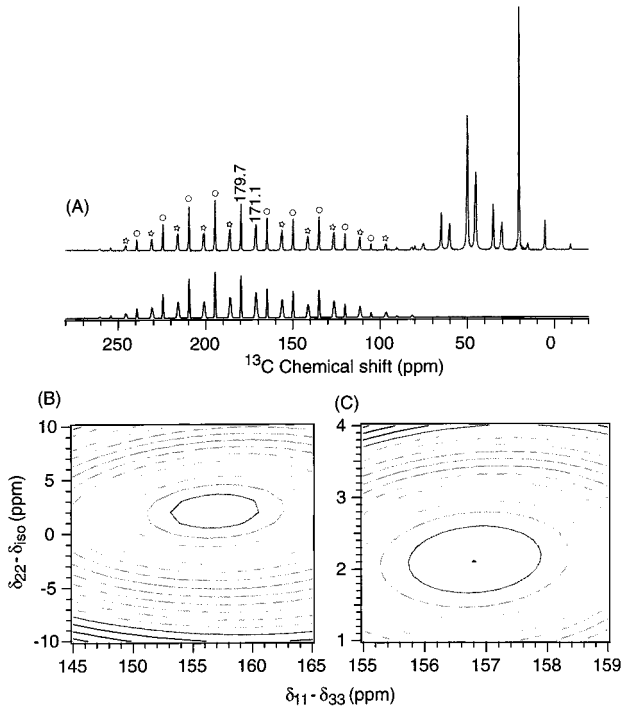

Figure 1. (A) One-dimensional ^{13}C CPMAS spectrum of Ala-Gly powder sample obtained at a spinning speed of 1.5 kHz. The circles and stars indicate spinning sidebands that correspond to the ^{13}-Carboxylate of glycine and the ^{13}Carbonyl of alanine residues of the Ala-Gly dipeptide, respectively. The best-fitting simulated ^{13}C spinning sideband patterns are shown under the experimental spectrum. (B) The RMSD contour plot for the ^{13}Carbonyl of alanine obtained by varying CSA span Δ (defined as $\delta_{11} - \delta_{33}$) from 145 to 165 ppm and $\delta_{22} - \delta_{iso}$ from -10 to 10 ppm. The minimum RMSD value is normalized to 1.0. The innermost contour level is 1.5 and the contour interval is 0.5. (C) The contour plot in (B) is expanded in the range of 155−159 ppm for Δ and 1−4 ppm for $\delta_{22} - \delta_{iso}$. The minimum RMSD value represented by the center point is normalized to 1.0 and the contour interval is 0.05.

simulations;[45] where β_C is the angle between the most deshielded element δ_{11} and C_α−N bond and α_C is the angle between the projector of C_α−N vector on to the δ_{22}-δ_{33} plane and the δ_{33} axis. The magnitudes of the principal elements of the carbonyl carbon CSA tensors were measured from the ^{13}C CPMAS spectra of powder samples obtained at a spinning speed of 1.5 kHz. The spinning sidebands were simulated using the ^{13}C(O)−^{14}N dipolar coupling constant of 1260.3 Hz (for a C(O)−N bond length of 1.34 Å), and the angles that define the orientation of the ^{13}CO CSA tensor with respect to the ^{13}C(O)−^{14}N dipolar coupling, $\alpha_C = 90°$ and $\beta_C = -40°$.[8] The effects of the ^{13}C−^{14}N dipolar coupling on the ^{13}C CSA line shape were taken into account as described in the literature.[45, 46]

Results

Carbonyl ^{13}C CSA Tensors. The magnitudes of the principal elements of the ^{13}C(O) CSA tensor can be measured easily from the 1D ^{13}C CPMAS spectrum obtained at a low spinning speed (ca. 1.5−2.0 kHz in a 400 MHz spectrometer). A typical 1D ^{13}C CPMAS spectrum of the Ala-Gly dipeptide obtained at a spinning speed of 1.5 kHz is shown in Figure 1A. The peak at 179.7 ppm is assigned to the ^{13}Carboxylate group of the glycine residue and the peak at 171.1 ppm is assigned to the ^{13}Carbonyl group of the alanine residue of the Ala-Gly dipeptide. The sideband pattern was simulated for each peak to obtain the principal values of the CSA tensor as explained in the Experimental Section of the paper. The simulated spinning sideband patterns of the ^{13}CO and ^{13}COO$^-$ groups of the Ala-Gly dipeptide are shown in Figure 1A under the experimental spectrum, and the principal values of the CSA tensors are listed in Table 1. The errors for simulations were estimated using RMSD contour plots. Figure 1B is the RMSD contour plot for the ^{13}Carbonyl of alanine residue obtained by varying Δ (defined as $\delta_{11} - \delta_{33}$) from 145 to 165 ppm and $\delta_{22} - \delta_{iso}$ from -10 to 10 ppm. The minimum RMSD value is normalized to 1.0. The innermost contour level is 1.5 and the contour interval is 0.5. The range of 155−159 ppm for Δ and 1−4 ppm for $\delta_{22} - \delta_{iso}$ is expanded into Figure 1C. The minimum RMSD value represented by the center point is normalized to 1.0 and the contour interval is 0.05. The errors for Δ and $\delta_{22} - \delta_{iso}$ were estimated using the contour level of 5% more than the minimum RMSD value.

Carbonyl CSA tensors of small peptides and proteins have been reported extensively by using both solid-state and solution NMR methods. The isotropic carbonyl chemical shifts have been found to correlate with backbone amide hydrogen bonding in glycine,[47] alanine,[12] valine,[48] leucine,[48] and asparagine residues.[48] It has also been reported that the chemical shift tensors of the carbonyl carbons are strongly correlated with the hydrogen bonding.[14] The principal values of ^{13}Carbonyl CSA tensors associated with alanine and glycine residues determined in this study and from previous studies[8,9,12] are presented in Table 1. The CO···HN hydrogen bond distances obtained from crystallographic studies are also given in Table 1. Crystal structures were obtained from the Cambridge Structural Database[49−51] and from the following references: Ala-Gly;[52] Ala-Asp;[53] Ala-Ser;[54] Ala-Ala-Ala;[55] Ac−Ala−NHMe;[56] Ala-Gly-Gly·H_2O;[57] poly-L-alanine;[58−60] Gly-Ala;[61] Ac-Gly-Ala−NH_2;[62] Gly-Gly;[63] Gly-Gly·HNO_3;[64] Ac-Gly-Gly;[65] Val-Gly-Gly;[66] polyglycine.[67,68]

(45) Heller, J.; Laws, D. D.; Tomaselli, M.; King, D. S.; Wemmer, D. E.; Pines, A.; Havlin, R. H.; Oldfield, E. *J. Am. Chem. Soc.* **1997**, *119*, 7827−7831.
(46) Tycko, R.; Weliky, D. P.; Berger, A. E. *J. Chem. Phys.* **1996**, *105*, 7915−7930.
(47) Ando, S.; Ando, I.; Shoji, A.; Ozaki, T. *J. Am. Chem. Soc.* **1988**, *110*, 3380−3386.
(48) Tsuchiya, K.; Takahashi, A.; Takeda, N.; Asakawa, N.; Kuroki, S.; Ando, I.; Shoji, A.; Ozaki, T. *J. Mol. Struct.* **1995**, *350*, 233−240.
(49) Allen, F. H.; Bellard, S.; Brice, M. D.; Cartwright, B. A.; Doubleday: A.; Higgs, H.; Hummelink, T.; Hummelinkpeters, B. G.; Kennard, O.; Motherwell, W. D. S.; Rodgers, J. R.; Watson, D. G. *Acta Crystallogr. Sect. B−Struct. Commun.* **1979**, *35*, 2331−2339.
(50) Allen, F. H.; Kennard, O.; Taylor, R. *Accounts Chem. Res.* **1983**, *16*, 146−153.
(51) Allen, F. H.; Kennard, O. *Chem. Des. Automat. News* **1993**, *8*, 1 & 31−37.
(52) Koch, M. H. J.; Germain, G. *Acta Crystallogr., Sect. B* **1970**, *B 26*, 410.
(53) Eggleston, D. S.; Hodgson, D. J. *Int. J. Pept. Protein Res.* **1983**, *21*, 288−295.
(54) Jones, P. G.; Falvello, L.; Kennard, O. *Acta Crystallogr., Sect. B* **1978**, *34*, 1939−1942.
(55) Fawcett, J. K.; Camerman, N.; Camerman, A. *Acta Crystallogr., Sect. B* **1975**, *B 31*, 658−665.
(56) Harada, Y.; Iitaka, Y. *Acta Crystallogr., Sect. B* **1974**, *B 30*, 1452−1459.
(57) Lalitha, V.; Subramanian, E.; Bordner, J. *Indian J. Pure Appl. Phys.* **1985**, *23*, 506−508.
(58) Arnott, S.; Wonacott, A. J. *J. Mol. Biol.* **1966**, *21*, 371-&.
(59) Arnott, S.; Dover: S. D.; Elliott, A. *J. Mol. Biol.* **1967**, *30*, 201−208.
(60) Arnott, S.; Dover: S. D. *J. Mol. Biol.* **1967**, *30*, 209−212.
(61) Wang, A. H. J.; Paul, I. C. *Cryst. Struct. Commun.* **1979**, *8*, 269−273.
(62) Puliti, R.; Mattia, C. A. *Acta Crystallogr., Sect. C* **1995**, *51*, 336−339.
(63) Kvick, A.; Alkaraghouli, A. R.; Koetzle, T. F. *Acta Crystallogr., Sect. B* **1977**, *33*, 3796−3801.
(64) Rao, S. N.; Parthasa. R *Acta Crystallogr., Sect. B* **1973**, *B 29*, 2379−2388.
(65) Rao, S. T. *Cryst. Commun.* **1973**, *2*, 257.

Table 1. Magnitudes of Carbonyl ^{13}C CSA Tensors in Peptides

compound	$\delta_{iso\ (ppm)}$	$\delta_{11\ (ppm)}$	$\delta_{22\ (ppm)}$	$\delta_{33\ (ppm)}$	Δ (ppm)[a]	CO···HN (Å)
			Alanine Residues			
*Ala-Gly	171.1	248.5 ± 0.8	173.2 ± 0.5	91.6 ± 0.8	156.9 ± 1.1	*f*
*Ala-Asp	171.7	247.4 ± 2.5	177.5 ± 2.0	90.2 ± 2.5	157.2 ± 3.0	2.975
*Ala-Ser	170.4	245.5 ± 3.0	170.8 ± 2.5	94.9 ± 3.0	150.6 ± 3.5	3.035
Ala-*Ala-Ala	172.0	250.2 ± 1.6	175.5 ± 1.0	90.3 ± 1.6	159.9 ± 2.2	2.915
PLA (α-helix)	176.6	251.8 ± 1.8	185.2 ± 1.1	92.8 ± 1.8	159.0 ± 2.5	2.87
PLA (β-sheet)	173.1	248.3 ± 1.0	180.1 ± 0.5	90.9 ± 1.0	157.4 ± 1.5	2.83
Ac-*AlaNHMe[b]	175.9	245	186	96	149	2.92
	177.0	241	196	94	147	2.72
*AlaGlyGly·H_2O[b]	172.6	245	179	93	152	3.00
			Glycine Residues			
*Gly-Ala	166.4	248.8 ± 0.8	159.9 ± 0.5	90.5 ± 0.8	158.3 ± 1.1	*f*
Ac*GlyAlaNH_2[c]	172.2	242.0	184.8	89.9	152.1	2.872
*Gly-Gly[d]	168.1	242.3	173.8	88.2	154.1	2.97
*Gly-Gly·HNO_3[d]	168.3	248.1	167.8	89.1	159.0	3.12
Ac-*Gly-Gly	170.1	244	176	91	170	2.82
Ala-*Gly-Gly	170.6	240	177	94	146	2.93
Val-*Gly-Gly[e]	169.2	245	170	93	152	3.05
PolyGly β-sheet	169.6	245	173	91	154	2.91
PolyGly 3_1-helix	173.2	247	182	91	156	2.73

[a] $\Delta = \delta_{11} - \delta_{33}$. The errors for the data measured from this study were estimated based on RMSD plots (see the text for details). [b] Reference 12. [c] Reference 8. [d] Reference 9. [e] Reference 14. [f] Crystal structures show no intermolecular backbone CO···HN hydrogen bonds.

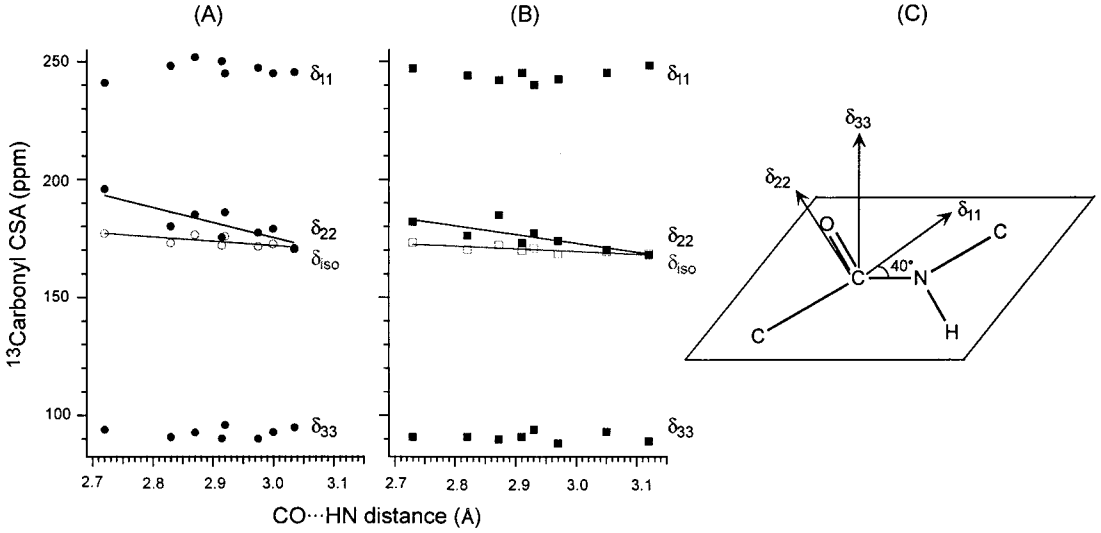

Figure 2. Dependence of ^{13}Carbonyl chemical shift tensor against the intermolecular CO···HN hydrogen-bonding distance in peptides for alanine residues (A) and glycine residues (B). Open symbols represent the isotropic chemical shifts, while filled symbols represent the magnitudes of the principal components of the CSA tensor. The δ_{22} tensor element is strongly correlated to the hydrogen bonding for both alanine and glycine residues, while δ_{11} and δ_{33} are insensitive to the variation in the hydrogen-bonding length. (C) Typical orientation of the ^{13}Carbonyl CSA tensors in a peptide plane. The δ_{33} axis is perpendicular to the peptide plane, whereas δ_{22} and δ_{11} axes are in the peptide plane. The δ_{22} axis is close to the C═O bond vector, while δ_{11} axis is approximately perpendicular to the C═O bond and makes ~40° with the C−N bond vector.

The dependence of the principal values of ^{13}CO CSA tensors against the length of the CO···HN hydrogen bond is shown in Figure 2 along with a typical orientation of the ^{13}CO CSA tensor in a peptide plane. For both alanine and glycine residues (Figure 2, A and B, respectively), the isotropic chemical shifts show a weak correlation with the hydrogen bonding: as the hydrogen bond length decreases the isotropic chemical shift slightly shifts downfield. The isotropic chemical shifts vary about 10 ppm as the hydrogen bond length changes from 2.72 to 3.12 Å. The linear correlations between the isotropic ^{13}CO chemical shift and the hydrogen bond length based on our experimental data can be expressed as

$$\delta_{iso}\,(\mathrm{Ala}) = 227.0 - 18.3 \times R_{N\cdots O}\,(\mathrm{ppm}) \quad (R = -0.75)$$

$$\delta_{iso}\,(\mathrm{Gly}) = 204.3 - 11.7 \times R_{N\cdots O}\,(\mathrm{ppm}) \quad (R = -0.81)$$

These equations agree very well with previous studies within experimental errors.[12, 47]

Among all three principal elements of the ^{13}CO CSA tensor, the δ_{22} is the most sensitive element, varying up to 30 ppm for alanine residues and up to 15 ppm for glycine residues for a change in the hydrogen-bonding distance from 2.72 to 3.12 Å. This can be attributed to the fact that the orientation of the δ_{22} element is in the peptide plane and is very close to the C═O bond vector (see Figure 2C). The trend is as expected that the δ_{22} values are more deshielded as the CO···HN distance

(66) Lalitha, V.; Murali, R.; Subramanian, E. *Int. J. Pept. Protein Res.* **1986**, *27*, 472−477.
(67) Lotz, B. *J. Mol. Biol.* **1974**, *87*, 169.
(68) Ramachandran, G. N.; Sasisekharan, V.; Ramakrishnan, C. *Biochim. Biophys. Acta* **1966**, *112*, 168.

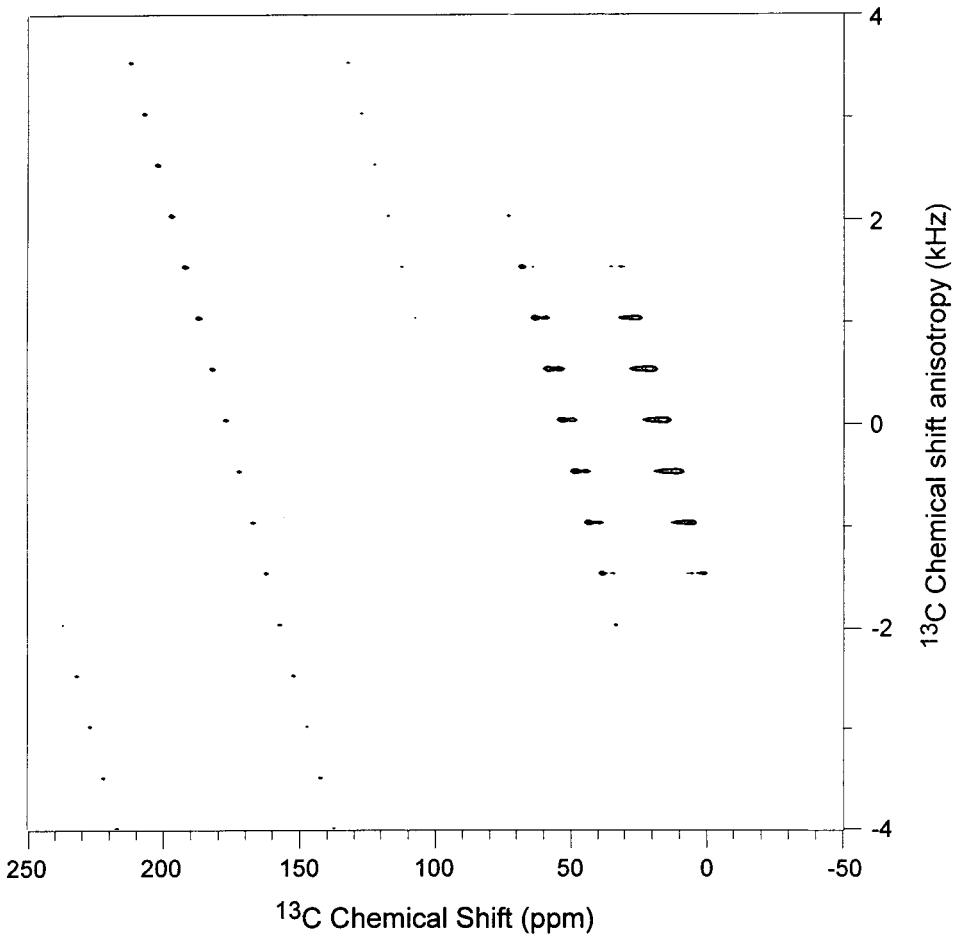

Figure 3. 2D-PASS spectrum of poly-L-alanine powder sample.

becomes shorter. The relations between the δ_{22} tensor element and the hydrogen bonding distance were determined by the least-mean squares method:

$$\delta_{22}\,(\text{Ala}) = 366.8 - 63.8 \times R_{\text{N}\cdots\text{O}}\,(\text{ppm}) \quad (R = -0.83)$$

$$\delta_{22}\,(\text{Gly}) = 285.0 - 37.4 \times R_{\text{N}\cdots\text{O}}\,(\text{ppm}) \quad (R = -0.81)$$

These expressions, within experimental errors, agree very well with previous studies.[14] As seen from the relationships for the δ_{iso} and δ_{22} in alanine and glycine residues, the hydrogen bonding dependence of the δ_{iso} and δ_{22} element is much larger in alanine than in glycine residues. Crystal structures show that there are no intermolecular CO···HN hydrogen bonds in Ala-Gly and Gly-Ala dipeptides.[52,61] The δ_{iso} and δ_{22} values for the carbonyl carbon of Gly-Ala set the lower limit (most shielded) for glycine residues in Table 1. Although the δ_{iso} and δ_{22} values for the carbonyl carbon of Ala-Gly are not the smallest, they are among the most shielded ones that are listed in Table 1. In these dipeptides, crystal packing may play a major role in the shielding tensors.

The δ_{11} and δ_{33} elements are much less sensitive to the hydrogen bonding than the δ_{22} element, varying only up to 10 ppm for the same hydrogen-bonding distance range for both alanine and glycine residues, and showing no trend. This can be rationalized that both the δ_{11} and δ_{33} elements are perpendicular to the C═O bond vector as shown in Figure 2C. Since the magnitudes of δ_{11} and δ_{33} elements are almost constant and have no trend within the normal hydrogen-bonding range, the variation in the spans of the CSA tensor (defined as $\Delta = \delta_{11} - \delta_{33}$) is negligible. The CSA spans are within the range of 145−160 ppm for glycine and alanine residues. The average anisotropy of ^{13}CO CSA, defined as $\delta_{11} - {}^1/_2(\delta_{22} + \delta_{33})$, was found to be 110.2 ± 6.6 ppm for alanine residues and 112.4 ± 6.4 ppm for glycine residues (the reported errors are standard deviations). These values are considerably smaller than those determined from many cross-correlated relaxation studies on water-soluble proteins using multidimensional solution NMR methods. Dayie and Wagner reported a wide range of carbonyl ^{13}C CSA in *villin 14T* protein, where the average anisotropy

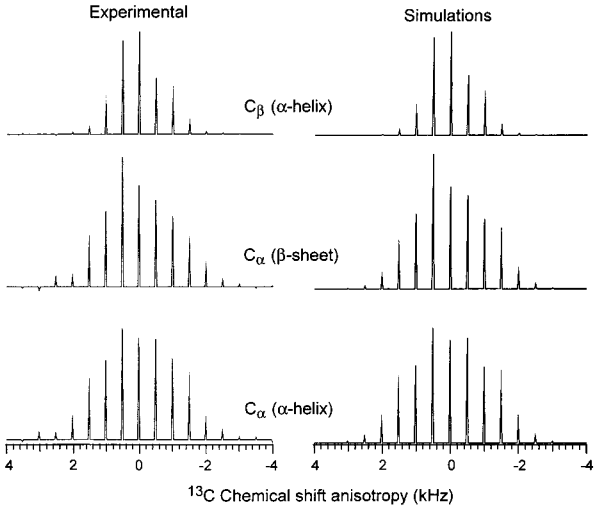

Figure 4. Experimental and the best-fitting simulated 1D spinning CSA sideband patterns of $^{13}C_\alpha$ and $^{13}C_\beta$ of poly-L-alanine powder sample. The experimental spectra were obtained from the 2D-PASS spectrum in Figure 3 after proper data-shearing for each t_1 increment.

Table 2. Magnitudes of ^{13}C CSA Tensors Associated with C_α and Side Chain Carbons in Peptides

compound	carbon site	δ_{iso} (ppm)	$\delta_{11} - \delta_{iso}$ (ppm)	$\delta_{22} - \delta_{iso}$ (ppm)	$\delta_{33} - \delta_{iso}$ (ppm)	CSA span Δ (ppm)[a]	η[a]
Poly-L-Ala	C_α (α-helix)	53.3	18.7 ± 0.5	-1.4 ± 0.3	-17.3 ± 0.5	36.0 ± 0.7	0.85 ± 0.07
	C_α (β-sheet)	48.9	15.7 ± 0.6	0.8 ± 0.4	-16.5 ± 0.6	32.2 ± 0.8	0.93 ± 0.10
	C_β (α-helix)	15.8	10.9	2.6	-13.5	24.4	0.61
Ala-Gly	Ala-C_α	49.8	8.9 ± 2.0	6.9 ± 1.8	-15.8 ± 2.0	24.7 ± 2.2	0.13 ± 0.26
	Ala-C_β	20.1	13.9	-0.1	-13.7	27.6	0.98
	Gly-C_α	45.0	21.6 ± 1.8	-1.3 ± 1.1	-20.3 ± 1.8	41.9 ± 2.5	0.88 ± 0.21
Gly-Ala	Gly-C_α	39.6	10.9 ± 3	6.2 ± 3	-17.1 ± 3	28.0 ± 3	0.27 ± 0.4
	Ala-C_α	53.2	14.6 ± 0.9	-0.7 ± 0.8	-13.9 ± 0.9	28.5 ± 1.0	0.90 ± 0.17
	Ala-C_β	16.7	11.5	3.9	-15.3	26.8	0.50
Ala-Asp	Ala-C_α	49.3	8.2 ± 1.5	6.6 ± 1.4	-14.8 ± 1.5	23.0 ± 1.6	0.11 ± 0.21
	Ala-C_β	16.3	11.4	1.3	-12.8	24.2	0.79
	Asp-C_α	52.7	19.1 ± 1.8	5.2 ± 1.3	-24.3 ± 1.8	43.4 ± 2.3	0.57 ± 0.17
	Asp-C_β	37.2	12.1	7.2	-19.3	31.4	0.25
N-acetyl-D,L-alanine	Acetyl-CH_3	22.1	18.5	4.3	-22.8	41.3	0.62
	Ala-C_α	49.8	17.4 ± 1.3	-1.0 ± 0.6	-16.4 ± 1.3	33.8 ± 2.0	0.88 ± 0.17
	Ala-C_β	19.2	16.9	-1.8	-15.1	32.0	0.79

[a] $\Delta = \delta_{11} - \delta_{33}$, $\eta = (\delta_{yy} - \delta_{xx})/(\delta_{zz} - \delta_{iso})$, assuming $|\delta_{zz} - \delta_{iso}| \geq |\delta_{xx} - \delta_{iso}| \geq |\delta_{yy} - \delta_{iso}|$. The errors were estimated based on RMSD plots (see the text for details).

values extend from 120 to 160 ppm.[16] Cornilescu and Bax determined the ^{13}CO average anisotropy values to be 141.7 ± 3 ppm for α-helix residues, 126.0 ± 6 ppm for β-sheet residues, and 129.8 ± 3 ppm for all residues in *ubiquitin*.[23] Recently, Pang and Zuiderweg measured ^{13}CO CSA tensors in *binase*, and the average anisotropy values were found to be 102.7 ± 6.62 ppm for α-helix residues, 103.6 ± 27.9 ppm for β-sheet residues, 108.4 ± 25.4 ppm for the residues in a loop, and 105.8 ± 27.0 ppm for all residues.[21] These values are similler to those reported from solid-state NMR studies but the dispersion is relatively large. The orientations of carbonyl CSA tensors determined from solution NMR studies are in excellent agreement with those measured from solid-state NMR studies, and the angles between the least shielded component δ_{11} and the C(O)−N bond vector were found to be $38 \pm 2°$ in *ubiquitin*[23] and $40.0 \pm 9.4°$ in *binase*.[21] The same angles measured from solid-state NMR range from 33 to 47°.[8, 9, 26]

C_α and Aliphatic Side Chain ^{13}C CSA Tensors. Since the span of ^{13}C CSA tensors of C_α and other aliphatic carbons are very small (~40 ppm or less), it is very difficult to obtain the magnitudes of the components of the CSA tensors accurately using a simple 1D ^{13}C CPMAS experiment. On the other hand, the two-dimensional PASS experiment on a powder sample provides a way to obtain spinning sideband patterns at a very low MAS speed (ca. 0.5−1.0 kHz). A typical 2D PASS spectrum is shown in Figure 3 for the poly-L-alanine (PLA) powder sample at a spinning speed of 500 Hz. In the 2D spectrum, the spinning sidebands are spread out in the 2D spectrum while the centerband is located in the center of the indirect dimension from which the isotropic chemical shift of each peak can be measured. After data shearing,[35] the ^{13}C CSA spinning sideband pattern can be obtained by taking a slice at an isotropic ^{13}C chemical shift peak along the indirect frequency dimension for each carbon site. Figure 4 shows the experimental and simulated ^{13}C CSA sideband patterns of C_α and C_β of the poly-L-alanine powder sample. The $^{13}C_\alpha-^{14}N$ dipolar coupling of 712.7 Hz for a bond length of 1.45 Å, which is comparable to the spinning speed of the experiment, is expected to have a significant effect on the ^{13}C CSA line shapes obtained from the 2D PASS experiment. Therefore, the magnitude of the $^{13}C_\alpha-^{14}N$ dipolar coupling and its orientation relative to the $^{13}C_\alpha$ CSA tensor were taken into account in the simulations of $^{13}C_\alpha$ CSA spinning sideband patterns as described elsewhere.[45,46] Since a C_β carbon is normally far away from ^{14}N in a peptide, the effect of $^{13}C_\beta-^{14}N$ dipolar coupling was not considered in the simulations of $^{13}C_\beta$ CSA spinning sideband patterns. These experimental and simulation procedures were carried out on powder samples of several peptides. The traceless principal values of the ^{13}C CSA tensors ($\delta_{ii} - \delta_{iso}$) are given in Table 2. In Table 2, CSA span Δ is defined as $\delta_{11} - \delta_{33}$, and η is defined as $(\delta_{yy} - \delta_{xx})/(\delta_{zz} - \delta_{iso})$, assuming $|\delta_{zz} - \delta_{iso}| \geq |\delta_{xx} - \delta_{iso}| \geq |\delta_{yy} - \delta_{iso}|$. For C_α carbons, the errors on Δ and traceless anisotropic tensor values were estimated using the 2D RMSD plots that were generated by comparing simulated spectra with experiments for various values of Δ and $\delta_{22} - \delta_{iso}$. For example, the RMSD contour plots for the ^{13}C CSA of C_α of poly-L-alanine are shown in Figure 5.

Two different types of $^{13}C_\alpha$ CSA tensors were identified in small peptides. The CSA tensors of $^{13}C_\alpha$ in the first residue of peptides, which are located near the N-terminal of the peptide, are similar but different from the $^{13}C_\alpha$ CSA tensors of $^{13}C_\alpha$ in the second or later residues of the peptide. For example, the $^{13}C_\alpha$ CSA spinning sideband patterns for these two types of C_α carbons of an Ala residue in Ala-Gly and Gly-Ala dipeptides are clearly different as shown in Figure 6. The alanine C_α carbon in the Ala-Gly dipeptide shows a ^{13}C CSA sideband pattern close to axial symmetry, in which η is close to 0, while the alanine C_α carbon in Gly-Ala dipeptide shows a highly asymmetric ^{13}C CSA pattern, where η is close to 1. By simulating the spinning sideband patterns as shown in Figure 6B, we obtained a series of CSA span Δ and asymmetric parameter η for various peptides. In general, the C_α carbons located in the first residue of a peptide tend to have a smaller Δ value ($\Delta < 28$ ppm) and a very small η value ($\eta < 0.3$), while the ones located in the second or later residues have a larger Δ value ($\Delta > 28$ ppm) and a η value close to 1. These two types of α-carbons fall into two distinct regions in the plot η against Δ (Figure 7).

The CSA tensors of C_β carbon mainly depend on the side chain conformation or the χ dihedral angles of residues, and the dynamics of the side chain. For alanine residues, the conformation and the dynamics of the side chain are relatively simple, and the CSA tensors for alanine C_β carbon have no clear trends in terms of the span of the CSA and the anisotropic parameter (Table 2). Since the methyl group in L-alanine amino acid rotates with a frequency of $\sim 10^8$ Hz around the C_{3v} axis,[69] an axially symmetric $^{13}C_\beta$ CSA tensor may be predicted for alanine residues in peptides and proteins. The results in Table

(69) Beshah, K.; Olejniczak, E. T.; Griffin, R. G. *J. Chem. Phys.* **1987**, *86*, 4730−4736.

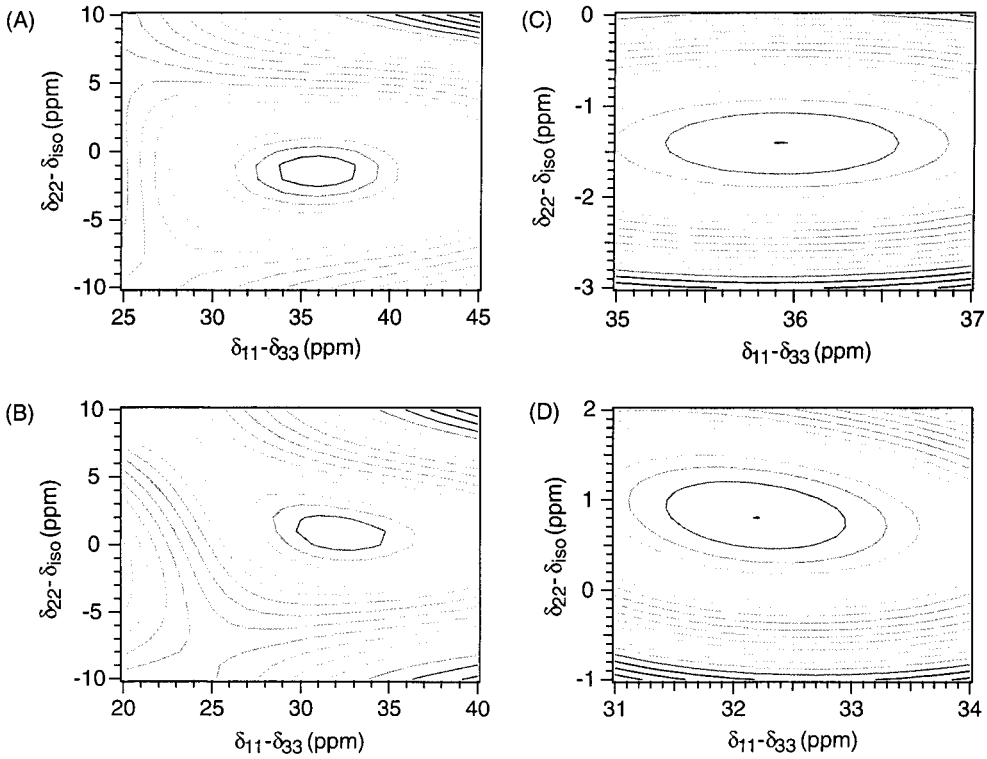

Figure 5. The RMSD contour plots that represent the errors in the measurement of $^{13}C_\alpha$ chemical shifts from poly-L-alanine powder sample. The plots (A) and (C) are for the α-helix conformation, and the plots (B) and (D) are for the β-sheet conformation of poly-L-alanine. The plots (A) and (B) were obtained by comparing the experimental spectra with the simulated spectra that were generated by varying Δ (defined as $\delta_{11} - \delta_{33}$) from 20 to 45 ppm, and $\delta_{22} - \delta_{iso}$ from −10 to 10 ppm. The minimum RMSD value is normalized to 1.0. The innermost contour level is 1.5, and the contour interval is 0.5. The plots (C) and (D) are expansions of the plots (A) and (B), respectively. The minimum RMSD value represented by the center point is normalized to 1.0, and the contour interval is 0.05.

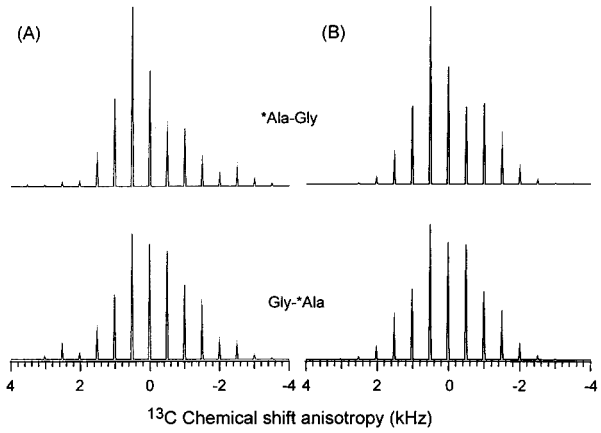

Figure 6. The spinning CSA sideband patterns for C_α carbons of alanine residues at different position of dipeptides. (A) and (B) are experimental and simulated spectra, respectively. The experimental spectra were obtained from 2D PASS spectra of Ala-Gly and Gly-Ala dipeptides (spectra not shown). The C_α CSA powder pattern is axially symmetric for the Ala residue in the first position, that is for the Ala-Gly dipeptide, while the CSA powder pattern is highly asymmetric for the Ala residue in the second position, that is for the Gly-Ala dipeptide. This trend was also observed for the CSA sideband patterns of C_α carbons in nonterminal residues of a peptide.

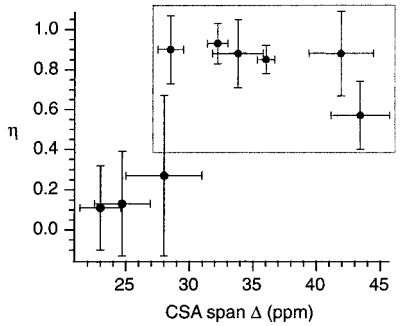

Figure 7. A plot of η (defined as $(\delta_{yy} - \delta_{xx})/(\delta_{zz} - \delta_{iso})$) versus CSA span Δ (defined as $\delta_{11} - \delta_{33}$) for the CSA of C_α carbons in peptides. Two types of C_α carbons can be distinguished in the $\eta - \Delta$ plot, in which the lower left region ($\eta < 0.3$, $\delta < 28$ ppm) is for the residues in the first position, while the upper-right region ($\eta > 0.5$, $\delta > 28$ ppm) is for the residues in the second or later positions of a peptide. The error bars were estimated from the 5% RMSD contour level.

2 suggest that this prediction need not be true for all peptides. For example, the $^{13}C_\beta$ CSA tensors of Ala residues in Ala-Gly, Ala-Asp and *N*-acetyl-D,L-alanine peptides are highly asymmetric ($\eta = 0.79-0.98$) while they are more symmetric in poly-L-Ala and Gly-Ala peptides ($\eta = 0.50-0.61$), but none of them are really axially symmetric ($\eta \approx 0$). These results suggest that packing interactions in the solid-state could have a significant effect on the asymmetry as well as on the span of the $^{13}C_\beta$ CSA tensors of alanine residues of peptides. The CSA tensors of C_β carbons of bigger and more complex amino acids may have larger variations due to the fact that the side chain can adopt more conformations, degrees of motions, and hydrogen bonding. The electrostatic effects may further complicate the analyses of CSA for hydrophilic and charged residues. Taking the Ala-Asp dipeptide as an example, the span of the CSA tensor for the C_β carbon of the aspartic acid residue is larger (31.4 ppm) than that of alanine (~25 ppm), and the CSA pattern is close to axially symmetric ($\eta = 0.25$). Therefore, the CSA tensors of side chain carbons are important in understanding the structure, dynamics, and function of peptides and proteins.

Table 3. Comparison of the Magnitudes of $^{13}C_\alpha$ CSA Tensors in Amino Acids, Peptides, and Proteins

compound	δ_{iso}	δ_{11}	δ_{22}	δ_{33}	$\Delta\delta$[a]	η[a]	ref
glycine	43.5	61 ± 3	46 ± 1	24 ± 5	30 ± 12	0.75	70
alanine	50.9	63 ± 1	56 ± 1	30 ± 3	30 ± 8	0.32	
aspartic acid	53.8	68 ± 2	56 ± 2	38 ± 2	24 ± 6	0.75	
A*AA[b]	49.6	70.2 ± 0.2	54.9 ± 0.2	23.6 ± 0.4	39.0	0.59	45
	149.02	132.93	148.20	165.92	25.4	0.90	
A*AA- hemihydrate[b]	50.3	71.0 ± 1.2	55.8 ± 1.6	24.0 ± 2.8	39.5	0.58	
	149.12	133.75	148.95	164.65	23.3	0.98	
G*AV[b]	52.6	76.9 ± 0.04	55.4 ± 0.05	25.5 ± 0.09	40.6	0.79	
	146.70	129.45	146.18	164.46	26.6	0.94	
PLA (α)[b]	52.7	72.1	54.3	31.7	31.5	0.85	33
	155.69	138.40	159.16	169.52	25.9	0.60	
PLA (β)[b]	48.6	59.7	54.6	31.6	25.5	0.65	
	156.58	143.68	152.33	173.73	25.7	0.50	
PLA (α)	53.3	72.0	51.9	36.0	28.0	0.85	this work
PLA (β)	48.9	64.6	49.7	32.4	24.8	0.90	
*Gly-Ala	39.6	50.5	45.8	22.5	25.6	0.27	
Gly-*Ala	53.2	67.8	52.5	39.3	21.9	0.90	
NA*A	49.8	67.2	48.8	33.4	26.1	0.89	
*Ala-Gly	49.8	58.7	56.7	34.0	23.7	0.13	
Ala-*Gly	45.0	66.6	43.7	24.7	32.4	0.88	
*Ala-Asp	49.3	57.4	55.9	34.5	22.2	0.10	
Ala-*Asp	52.7	71.8	57.9	28.4	36.4	0.57	
glycine					34 ± 3	0.4	15
glycine (α)	150.9	129.5	156.2	166.9	32.1	0.50	34
glycine (β)	155.2	141.3	150.6	173.7	27.8	0.50	
alanine (α)	145.9	129	147.9	160.7	25.4	0.75	
alanine (β)	150.9	134.6	152.7	165.3	24.5	0.77	
valine (α)[c]	136.3	126.1	136.3	146.5	15.3	1.00	
valine (β)[c]	142.1	122.0	147.2	157.3	30.2	0.50	
isoleucine (α)[c]	136.2	128.1	133.7	146.8	15.9	0.53	
isoleucine (β)[c]	140.6	118.8	147.3	155.8	32.7	0.39	
serine (α)	137.4	125.7	136.7	149.9	18.8	0.88	
serine (β)	144.7	128.3	148.6	157.3	24.6	0.53	
threonine (α)[c]	136.1	126.9	136.6	144.8	13.8	0.84	
threonine (β)[c]	142.0	123.8	146.0	156.1	27.3	0.55	
solution (α)[d]					6.1 ± 4.9		25
solution (β)					27.1 ± 4.3		

[a] $\Delta\delta = \delta_{zz} - {}^1/_2(\delta_{xx} + \delta_{yy})$, $\eta = (\delta_{yy} - \delta_{xx})/(\delta_{zz} - \delta_{iso})$, assuming $|\delta_{zz} - \delta_{iso}| \geq |\delta_{xx} - \delta_{iso}| \geq |\delta_{yy} - \delta_{iso}|$, except for data obtained from solution NMR. [b] The second set of data is obtained from ab initio calculations from the same reference. [c] The tensor values are the average at different χ angles. [d] Data from proteins *ubiquitin* and *calmodulin/M13*, $\Delta\delta = \delta_\perp - \delta_{||}$.

Discussion

To the best of our knowledge, only a few $^{13}C_\alpha$ tensors for amino acids, peptides, and proteins are available in the literature. Ye, et al. reported ^{13}C CSA tensors from amino acids in the solid-state.[70] Heller, et al. studied the $^{13}C_\alpha$ CSA tensors of alanine residue in a few short peptides using ^{13}C CPMAS method and ab initio calculations.[45] Havlin, et al. investigated $^{13}C_\alpha$ CSA of residues in different secondary structures and side chain conformations using quantum chemical simulations.[34] Asakawa, et al. reported ^{13}C chemical shift tensors for poly-L-alanine with different secondary structures using two-dimensional spin−echo NMR and ab initio shielding calculations.[33] Hong studied CSA decay curves using CSA-filter experiments for amino acids and ubiquitin protein in solid-state.[15] There is also a cross-correlated relaxation study on $^{13}C_\alpha$ CSA tensors from ubiquitin and calmodulin/M13 complex using high-resolution solution NMR experiments.[25] In Table 3, we have compiled the $^{13}C_\alpha$ CSA tensors that are available in the literature along with the data obtained from the present study. Conventionally, the tensor elements in Table 3 are defined as $\delta_{11} \geq \delta_{22} \geq \delta_{33}$. Ab initio studies reported the CSA tensors as chemical shielding, instead of chemical shift; these studies reported the CSA tensor elements according to the definition: $\delta_{33} \geq \delta_{22} \geq \delta_{11}$. In Table 3, the anisotropy ($\Delta\delta$) and the asymmetric parameter (η) were defined so that the asymmetric parameter varies between 0 and 1 for all solid-state NMR data and ab initio data: $\Delta\delta = \delta_{zz} - {}^1/_2(\delta_{xx} + \delta_{yy})$, $\eta = (\delta_{yy} - \delta_{xx})/(\delta_{zz} - \delta_{iso})$, assuming $|\delta_{zz} - \delta_{iso}| \geq |\delta_{xx} - \delta_{iso}| \geq |\delta_{yy} - \delta_{iso}|$. In solution NMR experiments, the anisotropy ($\Delta\delta$) value was not measured directly rather the difference between the perpendicular and parallel components of the CSA tensor projected on to the symmetry axis of the $^1H-^{13}C$ dipolar coupling tensor is reported. Therefore, the results obtained from solution NMR studies depend on $\Delta\delta$, as well as on the relative orientation of the CSA and dipolar coupling tensors, and on the asymmetry of the CSA tensor.

For free amino acids, the anisotropy $\Delta\delta$ is mostly in the range of 20−30 ppm (the sign of $\Delta\delta$ is ignored), but for some amino acids the $\Delta\delta$ value can be as low as 15 ppm, for example tyrosine, and as high as 38−41 ppm, for example leucine. The asymmetric parameter η is normally in the range of 0.70−1.00, but again, there are some exceptions, such as alanine (0.32), leucine (0.00), serine (0.59), glutamine (0.52), cysteine (0.47), and one of the tryptophan C_α peaks (0.40).[70] For small peptides, the asymmetric parameter is very small for the first residue of a peptide, indicating a highly asymmetric CSA pattern as explained before. On the other hand, the values of $\Delta\delta$ and η for the alanine residue located in the second or later positions in small peptides, or in a bigger polypeptide (like poly-L-alanine or a protein), are distinctly different from that of the first residues of peptides as shown in Figure 8. Various experimental and theoretical studies predicted that the $\Delta\delta$ value has a distribution of 20−32 ppm with the highest possibility around 25 ppm as illustrated in the histogram in Figure 8A, and most of the η values are very close to 1, indicating a highly asymmetric CSA

(70) Ye, C. H.; Fu, R. Q.; Hu, J. Z.; Hou, L.; Ding, S. W. *Magn. Reson. Chem.* **1993**, *31*, 699−704.

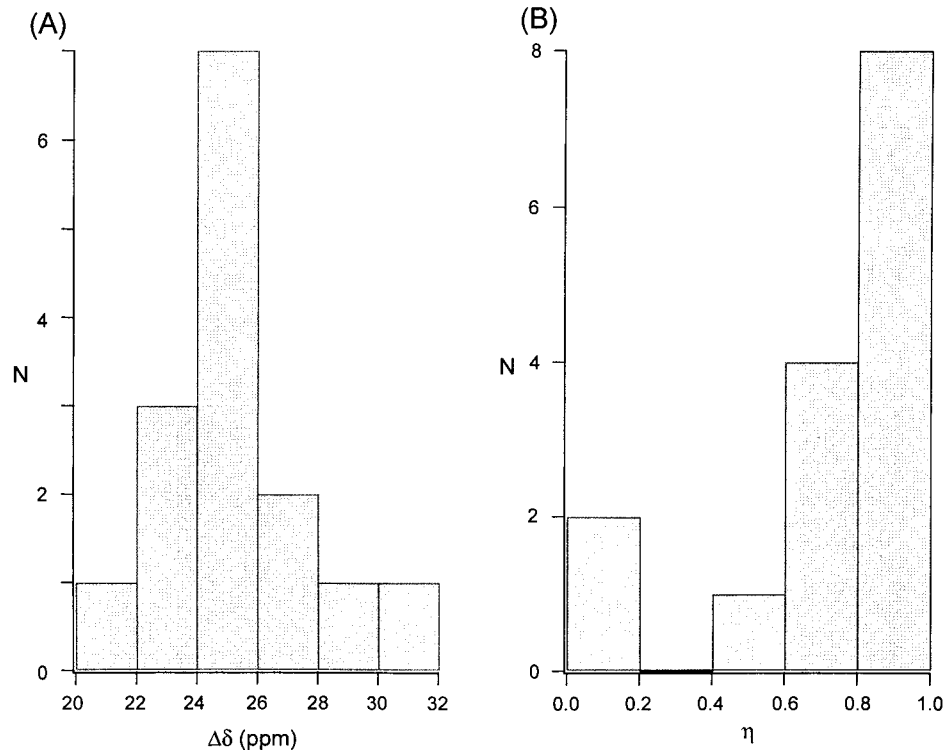

Figure 8. The histograms of the distributions of $\Delta\delta$ and η values for C_α carbons of alanine residues obtained from experiments and ab initio calculations in peptides and proteins (see Table 3). (A) The $\Delta\delta$ value is in the range of 20−32 ppm, and most populated at 24−26 ppm. It is worth mentioning that no significant variations were observed for alanine residues in α-helix and β-sheet conformations. (B) The η value covers the full range of 0−1. Those with very small η values (<0.2) are for the residues in the first position of a peptide, indicating axially symmetric CSA patterns. For other alanine residues, the η values are higher than 0.5, and most populated in the range of 0.8−1.0, indicating highly asymmetric CSA patterns. There are no significant differences for residues in α-helix and β-sheet conformations.

pattern (Figure 8B).[33,34,45] The only exception is the solid-state NMR study on tripeptides that reported $\Delta\delta$ to be around 40 ppm.[45] For alanine residues, the CSA anisotropy and asymmetric parameter are not sensitive to the backbone conformation and showed comparable values in both α-helix and β-sheet conformations, and in small peptides whose secondary structures are not well defined. Glycine residue in a peptide has a larger anisotropy ($\Delta\delta$ > 30 ppm) than the alanine residue, and a theoretical study showed that glycine residues in α-helix conformation have a larger CSA span than those in β-sheet conformation.[34] For amino acid residues other than glycine and alanine, however, trends of larger CSA tensor spans for sheet conformation over helix conformation is supported by ab initio study,[34] solution NMR cross-correlation relaxation study ($\delta_\perp - \delta_{||}$),[25] and recent solid-state CSA-filter experiments.[15]

The experimental and theoretical data indicated that $^{13}C_\alpha$ CSA tensor contains important information about protein secondary structure. Although ab initio shielding simulations have shown their successfulness in obtaining CSA tensor values and orientations,[71] it still requires experimental data as benchmark. Solution NMR studies based on cross correlation effects in water-soluble proteins enjoy high sensitivity and great resolution; however, solution NMR suffers from the intrinsic uncertainty in determining important CSA tensor parameters. Solid-state NMR has proven to be the most effective and accurate method in determining CSA tensors, but still it needs improvement in sensitivity and resolution. By combining the information from all different methods, we will have the capability to fully understand the variation of CSA tensors in proteins.

(71) deDios, A. C. *Prog. Nucl. Magn. Reson. Spectrosc.* **1996**, *29*, 229−278.

Conclusions

We have reported ^{13}C CSA tensors for several dipeptides and poly-L-alanine samples using 1D CPMAS and 2D PASS solid-state NMR experiments. The ^{13}Carbonyl CSA tensor was found to correlate with the backbone hydrogen-bonding distance, especially the δ_{22} tensor element is very sensitive to the hydrogen bonding distance. The $^{13}C_\alpha$ CSA tensor distinguishes the C_α carbons within and outside of a peptide plane in the way that the first residue in a peptide has relatively small CSA span (Δ < 28 ppm) and relatively axially symmetric sideband pattern (η < 0.3), while the rest of the residues have larger span (Δ > 28 ppm) and highly asymmetric CSA sideband patterns ($\eta \approx 1$). We have compared our data with previous experimental and theoretical studies on peptides and proteins, which indicate that $^{13}C_\alpha$ CSA tensors of alanine residues have little dependency on the protein secondary structure. The $^{13}C_\alpha$ CSA tensors of alanine can span from 20 to 30 ppm, but the most probable value is ∼25 ppm. Generally, the β-sheet residues have a larger CSA tensor span than the α-helix residues; however, a more detailed trend still awaits further scrutiny. We believe that the ^{13}C CSA tensors reported in this work will be highly useful in the structure and dynamics studies on the membrane-bound proteins using solid-state NMR methods and water-soluble proteins using solution NMR spectroscopy.

Acknowledgment. This work was supported in part by the research funds from NSF (CAREER Development Award to A.R.). Acknowledgment is also made to the donors of the Petroleum Research Funds, administered by the American Chemical Society, for partial support of this research.

JA010145L